Journal of Materials Chemistry

Cite this: J. Mater. Chem., 2012, 22, 19579

www.rsc.org/materials

PAPER

It takes walls and knights to defend a castle – synthesis of surface coatings from antimicrobial and antibiofouling polymers

Peng Zou,[ab] Wibke Hartleb[ab] and Karen Lienkamp*[ab]

Received 17th March 2012, Accepted 15th May 2012
DOI: 10.1039/c2jm31695a

The synthesis and characterization of a bifunctional material containing antimicrobial and antibiofouling components is presented. An end-functionalized antibiofouling poly(oxonorbornene)-based poly(zwitterion) was synthesized and grafted onto a surface-immobilized network of an antimicrobial poly(oxonorbornene), which is in this case a cationic synthetic mimic of an antimicrobial peptide (SMAMP). The resulting material was characterized by Fourier-transform infrared spectroscopy, ellipsometry, atomic force microscopy and surface plasmon resonance spectroscopy (SPR). The SPR data indicate that this bifunctional material is antibiofouling in spite of the underlying cationic SMAMP carpet, and as such it might be a promising material with potentially two lines of defense against biofilm formation.

Introduction

Biofilm formation is observed in many settings and in various dimensions, from plaque on teeth through catheters and medical devices to ship hulls, water purification systems and oil pipelines.[1] This has been discussed in a number of excellent papers and reviews (see ref. 1 and 2 and references therein). Biofilms are agglomerates of microorganisms that adhere to a substrate. The underlying processes and species involved are manifold, and so far the process has not been fully understood. According to a simplified mechanism, biofilm formation involves a number of steps: first, bacteria bind reversibly to a surface. They then secrete adhesion proteins, through which they can irreversibly attach.[2b] Alternatively, any proteins present in a specific setting, *e.g.* in body fluids, may adhere to a substrate, on which the bacteria subsequently settle.[3] Thus settled on the surface, the cells proliferate and form bacterial colonies inside a thick peptidoglycan envelope.[4] At this stage of biofilm formation, the bacteria become inaccessible to any antibacterial agents including disinfectants and antibiotics, as those molecules often cannot diffuse through the peptidoglycan layer. This is why biofilms in medical settings constitute a severe health threat, even where strict hygiene protocols are enforced. Therefore, materials that can effectively prevent biofilm formation in such high-infectious-risk settings are highly desirable as they may ease patient care and reduce infections with multiresistant bacteria.

The role of antibiofouling coatings is to prevent the transition from the reversible to the irreversible adhesive state of the cell. This can be achieved either by minimizing the adhesive forces between surface binding proteins and the substrate, or by enabling an easy detachment of the protein glue and the adhering microorganism from the surface (fouling-release coatings). In the former class of so-called non-biofouling or antibiofouling coatings, poly(ethylene glycol) (PEG) based surfaces have been the benchmark for years due to their low interfacial energy (5 mJ m^{-2}).[1,5] It has been argued that the hydration layer near the hydrophilic PEG surface was crucial to prevent protein adsorption, while the steric repulsion effect of long brush-like PEG chains would be negligible,[1] although other opinions also exist.[1,6] The drawback of PEG is that it degenerates oxidatively,[7] which is why alternatives are desirable.

Another class of antibiofouling polymers that constitutes a potential substitute for PEG are poly(zwitterions).[8] These polymers have equal numbers of negatively charged and positively charged moieties per repeat unit. Examples for zwitterionic polymers are poly(phosphorylcholines),[9] poly(sulfobetaines),[5h,10] and poly(carboxybetaines).[5h,10b,10c,11] Like PEG, these materials are extremely hydrophilic due to the association of large amounts of water around the charged groups. However, unlike poly(electrolytes), poly(zwitterions) do not perturb the hydrogen-bonded network of water near the surface, which is thought to prevent protein adsorption and biofouling.[12] Poly(zwitterions) were also found to have excellent biocompatibility towards fibroblasts and platelets,[11d] and help to reduce surface friction,[9i] protein adsorption, mammalian cell adhesion, and biofilm formation.[13]

On the downside, antibiofouling polymer surfaces are defenseless once bacteria have managed to settle on them, for example on surface inhomogeneities or other defects. However,

[a]*Department of Microsystems, Albert-Ludwigs-Universität Freiburg, Freiburg Institute for Advanced Studies (FRIAS), Albertstr. 19, Freiburg, Germany. E-mail: lienkamp@imtek.de; Fax: +49 761 203 7162; Tel: +49 761 203 7415*
[b]*Department of Microsystems Engineering (IMTEK), Georges-Köhler-Allee 103, Freiburg, Germany*

one bacterial cell may form a mature biofilm in less than 24 hours[14] and thereby cause severe inflammatory reactions on catheters or medical implants. Thus, for biomedical applications, another mechanism that can fight those settled bacteria would be desirable to obtain truly long-term biofilm-inert surfaces. This may be achieved by a combination of antibiofouling and antimicrobial polymers. Antimicrobial polymers kill airborne or solution-borne pathogens upon contact. Several examples of antimicrobial polymers have been reported, for example materials based on substituted poly(ethyleneimine), poly(vinylpyridine),[15,16] poly(diallyldimethylammonium),[17] poly(butylmethacrylate-*co*-aminoethyl methylacrylate),[18] and poly(2(dimethylamino)ethyl methacrylate)-based surfaces.[19] While the mechanism of action of antimicrobial polymers in solution is meanwhile partially understood,[20] the mechanism by which surface-bound polymers kill pathogens is still under debate.[15a,15d,18,19c,21] We have recently published a series of papers on so-called SMAMPs, which are synthetic mimics of antimicrobial peptides.[20n,22] These antimicrobial polymers are able to capture the key properties of the antimicrobial peptides (AMPs), which are host defense peptides and as such important components of the innate immune system. Like AMPs, our SMAMPs target the membranes of bacterial cells, where they presumably attach, insert, and then cause cell leakage and eventually cell death. While most antimicrobial polymers are generally biocidal, we showed that our poly(oxonorbornene)-based SMAMPs are selective for bacteria over mammalian cells. Thus, their potential toxicity for humans is low, which makes them attractive candidates as prospective materials in medical applications. However, antimicrobial materials including our SMAMPs are usually polycationic materials that strongly interact with anionic species including proteins, lipids and phospholipids. Consequently, they are also prone to quickly foul when used in "real-life" medical application.

Therefore, to overcome some of the above described drawbacks of purely antibiofouling or purely antimicrobial materials, we were interested in synthesizing a material from an antibiofouling poly(zwitterion) and an antimicrobial SMAMP. Such a material would have two lines of defense. First, the antibiofouling component would prevent bacterial adhesion as long as possible, like the walls of a castle hold back potential intruders. Then, when bacteria manage to settle and thereby come in close contact with the surface, they would be within reach of the antimicrobial components. In other words, when the walls are breached, the knights take action to defend the castle. There are only a few reports of simultaneously active antimicrobial and antibiofouling materials in the literature. Mostly, silver is embedded into a matrix of an antibiofouling polymer.[23] There are also a few cases of natural polyphenols with reportedly simultaneous antimicrobial and antibiofouling activity,[24] and in one case, a bifunctional membrane from antibiofouling poly(vinylidene fluoride) and antimicrobial poly[2-(*N*,*N*-dimethylamino)ethyl methacrylate] is described.[25] Further, poly(methacrylate)-based antimicrobials in combination with PEG in a network were reported.[26] Some very interesting work on a cationic polymer that can be hydrolyzed to yield antibiofouling poly(zwitterions) has also been reported, both for synthetic polymers and polysaccharide-based materials,[27] and very recently, the same group reported the incorporation of antibiotics in poly(zwitterions)[28] as well as a material which allowed reversible switching between an antimicrobial and an antibiofouling state.[29]

Here, we report how we synthesized a bifunctional material from a cationic antimicrobial poly(oxonorbornene)-based SMAMP and a zwitterionic antibiofouling poly(oxonorbornene) in a "grafting-onto" reaction. This material was carefully characterized using Fourier-transform infrared spectroscopy, ellipsometry, contact angle measurement, atomic force microscopy and surface plasmon resonance spectroscopy (SPR). In particular, we used surface plasmon resonance spectroscopy to demonstrate the presence of the thin poly(zwitterionic) layer. Preliminary SPR data that compare the surface-immobilized parent polymers (the cationic antimicrobial polymer network and the antibiofouling poly(zwitterionic) network) and the bifunctional material in terms of protein adhesion are also given.

Results

We present here the synthesis and characterization of a bifunctional material consisting of poly(cationic) antimicrobial SMAMPs and antibiofouling poly(zwitterions). A cartoon illustration of the design of our bifunctional target material is shown in Fig. 1. The bottom layer is a surface-immobilized network of the antimicrobial SMAMP (blue coil in Fig. 1), which was reacted with an end-functionalized antibiofouling poly(zwitterion) in a "grafting-onto" reaction (black zigzag line in Fig. 1).

This yields the desired material with short pendant antibiofouling groups on a thick carpet of SMAMP. To obtain this bifunctional material, we surface-immobilized the antimicrobial component on a model surface, using benzophenone as a crosslinker. The model surface was either a silicon wafer, or a gold substrate for the surface plasmon resonance measurements. It is well known that benzophenone reacts with any aliphatic CH moiety upon UV irradiation, which results in the formation of a covalent bond.[30] We therefore synthesized two linker molecules with a UV-crosslinkable benzophenone moiety and a surface-reactive site: a triethoxy benzophenone silane (3EBP, Fig. 2A) for the silicon wafer,[31] and a lipoic acid-derived benzophenone disulfide (DS, Fig. 2B) for the gold substrate. The reaction of these molecules with either silicon or gold yielded benzophenone-functionalized surfaces (Fig. 2).

Next, we synthesized the neutral precursor polymer **1** (Fig. 3) of the poly(oxonorbornene)-based SMAMP as reported

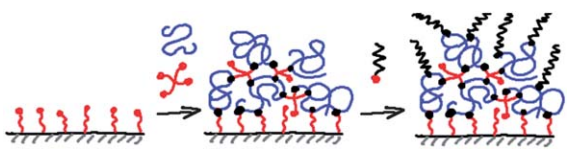

Fig. 1 Cartoon illustration: first, a model surface bearing benzophenone anchor groups (red curl) is coated with an antimicrobial polymer (blue coil) and a tetrafunctional thiol crosslinker (red cross, left). The red dots correspond to reactive groups. Upon UV irradiation, a surface-immobilized network is formed (black dots = covalent bonds). An antibiofouling polymer (black zigzag line) with a reactive end group is then grafted onto the antimicrobial polymer network to yield the target material (right).

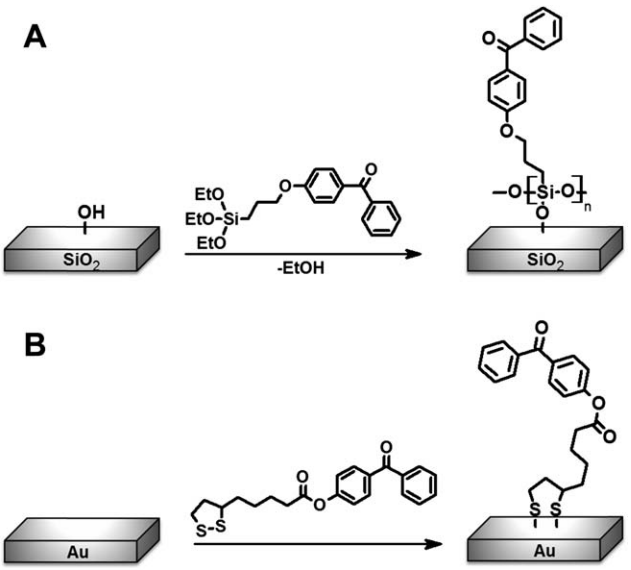

Fig. 2 Surface functionalization of a silicon wafer (A) and a gold surface (B) with a UV-sensitive benzophenone crosslinker.

previously.[22e] Using this neutral precursor polymer instead of directly using the cationic SMAMP was crucial to obtain the desired material, as the more hydrophilic SMAMP would invariably de-wet the benzophenone-functionalized surface. To obtain the SMAMP network, a solution of precursor polymer **1** was mixed with a tetrafunctional thiol cross-linker **2** and the UV sensitizer 2,2-dimethoxy-2-phenylaceto-phenone (DMPAP, **3**), and spin-coated onto the benzophenone-functionalized substrate (Fig. 3). Upon UV irradiation, the SH groups of cross-linker **2** and the double bonds of the precursor polymer **1** underwent a thiol–ene reaction (light dots in Fig. 3), while the emerging polymer network was simultaneously surface-immobilized through the benzophenone moieties (dark dots in Fig. 3). The Boc-protective group on the amine of the precursor polymer was then removed to yield the cationic, antimicrobially active SMAMP network.

Next, we synthesized the poly(zwitterion) as the antibiofouling component. To make this polymer react with the surface-immobilized SMAMP in a defined way, we needed to introduce a reactive functional group at the chain end. For that purpose, we made use of previously described end-functionalization chemistry.[22b] The Boc-protected zwitterionic monomer **4** was reacted with the pentafluorophenyl-functionalized quenching agent **5** to yield the end-functionalized, still Boc-protected precursor polymer of the antibiofouling polymer **6**, as shown in Fig. 4.

Next, the previously obtained SMAMP precursor network **7** was deprotected to yield the SMAMP network **8** (Fig. 5). After removal of the Boc-groups, the resulting ammonium groups of network **8** were converted into NH_2, which could then be used as an anchor group for the following "grafting-onto" reaction. Using classic peptide coupling chemistry (DMAP and dicyclohexylcarbodiimid), the pentafluorophenol active ester end group of the poly(zwitterion) precursor **6** was reacted with the polymer network **8**, forming an amide bond (**9**). Finally, treatment with HCl removed the protective group on the precursor polymer to yield the antibiofouling poly(zwitterion) grafts and turned the

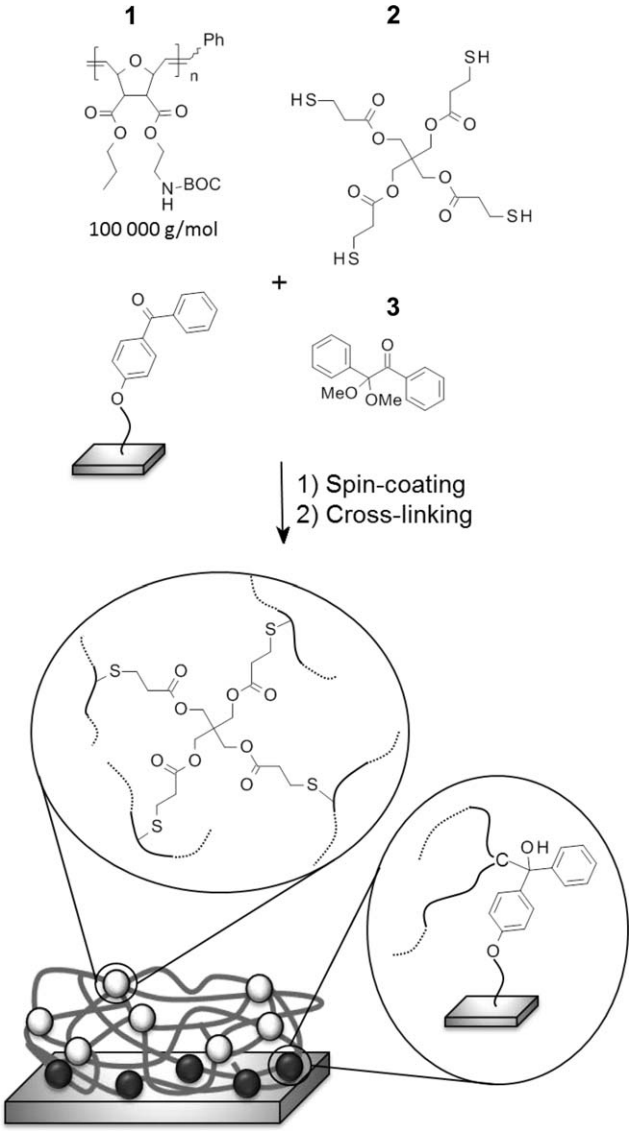

Fig. 3 SMAMP network synthesis: a solution containing the SMAMP precursor polymer **1**, the tetrafunctional thiol crosslinker **2** and the UV sensitizer (DMPAP) **3** was spin-coated onto a benzophenone-functionalized substrate. After cross-linking through UV irradiation, a surface-immobilized network was obtained.

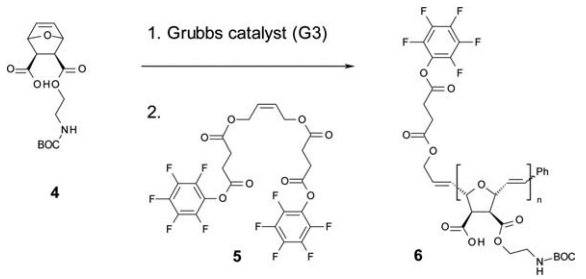

Fig. 4 Synthesis of the end-functionalized poly(zwitterion): the oxonorbornene monomer **4** was initiated with Grubbs' third generation catalyst. The living chain end was then quenched with a symmetric pentafluorophenylester-substituted 2-butenediol derivative **5** to yield the end-functionalized precursor polymer **6**.

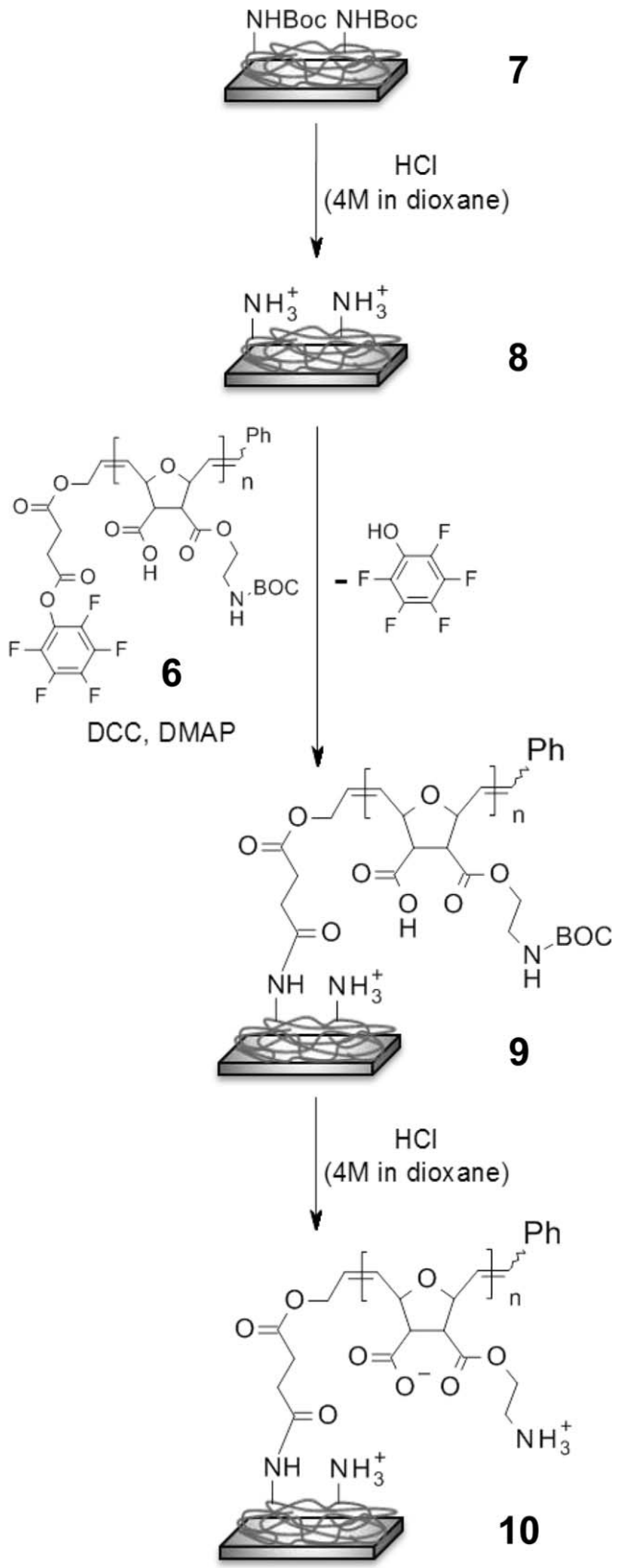

Fig. 5 After deprotection of the SMAMP precursor network **7** shown in Fig. 3, the end-functionalized poly(zwitterion) precursor **6** was grafted onto the SMAMP network **8**, yielding, after deprotection, the bifunctional target material **10**.

remaining amine groups of the SMAMP into antimicrobially active NH_3^+ groups (**10**, Fig. 5). With this last step, the target material, an antibiofouling poly(zwitterion) on a carpet of a cationic antimicrobial SMAMPs, was obtained.

At each step, the materials were characterized using ellipsometry, atomic force microscopy, Fourier-transform infrared spectroscopy and contact angle measurements. The results are summarized in Table 1. For comparison to the bifunctional material, we also synthesized and characterized a pure SMAMP network and a pure poly(zwitterion) network. The data obtained for these surface-immobilized networks are also included in Table 1. As can be seen from Table 1, the film thickness (obtained by ellipsometry and atomic force microscopy) decreased for all samples upon deprotection. This change can be understood as a relaxation of the network after removal of the bulky Boc-group. Alternatively, this effect might be due to the extraction of some material from the SMAMP layer that was either not covalently attached or whose attachment had suffered during the deprotection step. For the SMAMP network, a reduction from 49 nm to 36 nm was observed by ellipsometry. The "grafting-onto" procedure on this material increased the thickness to 48 nm, which was then further reduced to 37 nm after deprotection of the poly(zwitterionic) grafts. Thus, the overall thickness increase due to the grafts, according to ellipsometry, is only 1 nm. The same value was measured with AFM. On the one hand, this is plausible for grafts with a molecular mass of only 6000 g mol^{-1} – on the other hand, even though this value is confirmed by AFM it is also within the experimental error of ellipsometry. Further evidence was thus needed to confirm the success of the "grafting-onto" reaction. When comparing the contact angle data for the poly(zwitterion) with the data for the bifunctional material, a striking agreement is observed (Table 1), while the static, advancing and receding contact angles for the SMAMP are larger. This makes sense, as the SMAMP carries a propyl group where the poly(zwitterion) has a negative charge, *i.e.* the SMAMP is more hydrophobic. It is also in line with the proposed structure of the bifunctional material and indicates that the "grafting-onto" reaction was successful (or, at the very least, that a material with a poly(zwitterionic) top layer that could not be washed away was obtained).

Colak and Tew very recently reported a structurally related surface-immobilized poly(zwitterion), with contact angles of 36, 38 and 23° for the static, advancing and receding measurements.[13] Interestingly, for our material, the contact angle hysteresis was much larger. At the same time, the roughness of our materials was also larger, as revealed by AFM measurements (Table 1). When analyzing the AFM images (Fig. 6), we observed that we obtained a homogeneously cross-linked, surface immobilized network with pores of about 5 nm depth. This correlates well with the observed hysteresis in the contact angle, which hints at surface heterogeneities. The porous structure of our material was maintained even after significant chemical modification of the network, as the series of images in Fig. 6 illustrates. There is a slight increase in surface roughness after each reaction step, which is plausible, because each step involves chemical modification, swelling and drying of the material.

The FTIR data for the SMAMP and poly(zwitterion) networks are shown in Fig. 7a. Not surprisingly due to their close structural resemblance, the spectra of both protected networks

Table 1 Physical characterization data of the bifunctional material and the two model surfaces. Details are given in the Experimental section

		SMAMP		Poly(zwitterion)		Bifunctional material	
		Protected	Deprotected	Protected	Deprotected	Protected	Deprotected
Thickness (ellipsometry)/nm		49 ± 2	36 ± 2	40 ± 2	32 ± 2	48 ± 2	37 ± 2
Contact angle/°	Static	88 ± 3	56 ± 2	72 ± 2	54 ± 2	74 ± 2	54 ± 3
	Advancing	90 ± 2	59 ± 2	73 ± 2	59 ± 2	73 ± 2	58 ± 2
	Receding	38 ± 2	14 ± 2	14 ± 2	7 ± 2	16 ± 2	9 ± 2
AFM	Thickness /nm	40 ± 1	32 ± 1			37 ± 1	33 ± 1
	Roughness /nm	1 ± 0.5	2 ± 0.5			3 ± 0.5	4 ± 0.5

look very similar. In particular, they both have a broad absorption at 3400 cm^{-1} due to the stretch vibration of the NH bond from the Boc-protective group (arrow 1 in Fig. 7a). These bands disappear fully in the deprotected networks, indicating that the removal of the Boc-group is complete. The bands of the C═O stretch vibration in the carboxylic acid and ester of the poly(zwitterion) on the one hand, and the two ester groups in the SMAMP network on the other hand, are almost identical. However, there is a broad, low intensity band centered around 2600 cm^{-1} in the poly(zwitterion) spectrum (arrow 2 in Fig. 7a), which corresponds to the OH stretch of the free carboxylic acid. This peak also disappears in the deprotected poly(zwitterions) network because in this situation, the acid is deprotonated to the carboxylate, while the amine group is protonated. An overlay of the SMAMP network and the bifunctional material is shown in Fig. 7b. In these spectra, it can be also observed that the NH band of the Boc-group disappears after deprotection (arrow in Fig. 7b). Further interpretation is difficult due to the low amount of poly(zwitterionic) grafts relative to the underlying SMAMP. In comparison to the end-functionalized polyzwitterions before the "grafting-onto" reaction, however, it can be seen that the sharp C_6F_6 band of the active ester at 1520 cm^{-1} has vanished (see Experimental section, Fig. 10).

The ultimate proof of success of the "grafting-onto" reaction is to demonstrate the presence of antibiofouling properties of the material. To that end, we investigated the resistance of the material to protein adsorption using surface plasmon resonance spectroscopy (SPR). We chose two proteins and monitored their interaction with our three test surfaces (SMAMP network, poly-(zwitterion) network, and bifunctional material). In a typical protein adsorption experiment, a reflectivity baseline was recorded for 15 min. Then, the protein solution (bovine serum albumin (BSA) or fibrinogen in buffer) was injected into the SPR flow cell. After about 15 min, the flow cell was flushed with buffer to remove any non-adhering protein from the surface (this time point is marked with arrows in Fig. 8). Any protein that is irreversibly adsorbed on the surface would cause a shift in the resonance angle of the surface plasmon, leading to an increase of the reflectivity in the kinetic measurement. The results of the adsorption kinetics measurement for BSA are shown in Fig. 8a and those for fibrinogen are shown in Fig. 8b. In each case, the reflectivity change ΔR was plotted against time. Qualitatively, the results are similar for both proteins: while there is a huge change in reflectivity for the SMAMP surface after protein injection, the values for the poly(zwitterions) and the bifunctional surface are hardly affected. This corresponds to significant protein adhesion (fouling) on the SMAMP surface, and very little adhesion on the other two materials. Additionally, it was observed that the reflectivity values of both the poly(zwitterion) and the bifunctional surface return to the starting values after flushing the SPR cell with buffer. This indicates that these two surfaces are strongly antifouling. To quantify the amount of protein adhesion, we measured the thickness of the dry protein layer with SPR and compared this value to the one before protein exposure. On the SMAMP, a protein layer thickness of 5.9 nm was observed for BSA and 6.6 nm for fibrinogen, respectively. From $\rho = m\ V^{-1}$ and $V = t\ A$ (where ρ is the density of the protein, m its mass, and V its volume, t the measured dry thickness and A the surface area), the absorbed mass of protein per unit area can be calculated as $m\ A^{-1} = \rho\ t$.[13] Literature values for the density of the proteins are 1.085 g cm^{-3} for fibrinogen and 1.105 g cm^{-3} for BSA.[13] Thus, 6.52 ng mm^{-2} of BSA and 7.16 ng mm^{-2} of fibrinogen, respectively, were adsorbed on the SMAMP network. For the bifunctional material, the SPR curves obtained before and after the measurement are identical (Fig. 9). Thus, within the experimental error of this very sensitive method, no irreversible protein adsorption was observed.

The previously mentioned material by Colak and Tew[13] was also studied with respect to its antibiofouling properties. They measured the thickness of the material before and after protein adsorption to obtain the adsorbed amount of protein per unit area. For the best of their coatings, the protein adsorption was as low as 0.04 ng mm^{-2} (corresponding to an estimated protein thickness about 0.04 nm).[13] This is reportedly one of the best antibiofouling materials in the literature. We were hesitant to calculate the adsorbed protein thickness from our SPR data as the curves in Fig. 9 were so similar that any numerical difference between those curves would be well within the experimental error of the method. However, it seems that our bifunctional material is in a similar regime as those reported by Colak and Tew in terms of antibiofouling performance.

It goes without saying that further studies are needed to demonstrate the full antibiofouling potential of our material, where further protein experiments, adhesion experiments of bacterial cells, and long term activity experiments will be included.

Conclusion

We have presented here the synthesis and characterization of a novel bifunctional material, which consists of an antibiofouling and an antimicrobial polymer. The antimicrobial SMAMP was

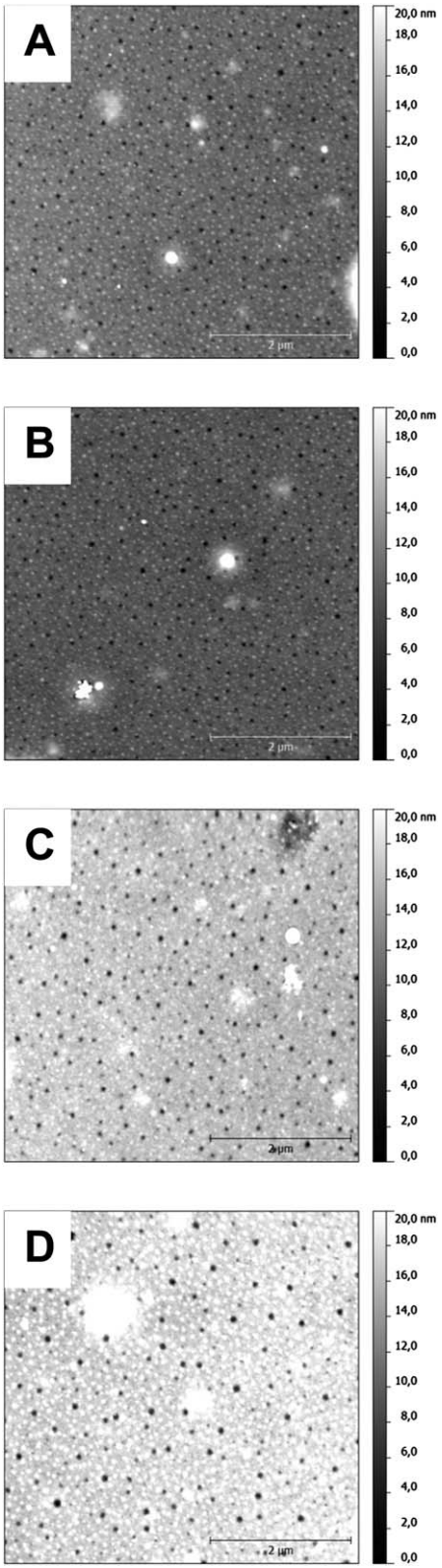

Fig. 6 AFM height images of the protected SMAMP network (A), the deprotected SMAMP network (B), the protected bifunctional material (C) and the deprotected bifunctional material (D). The images show that the overall porous network morphology is retained after each step, while the roughness slightly increases. Scale bar = 2 µm, *z*-scale = 0–20 nm.

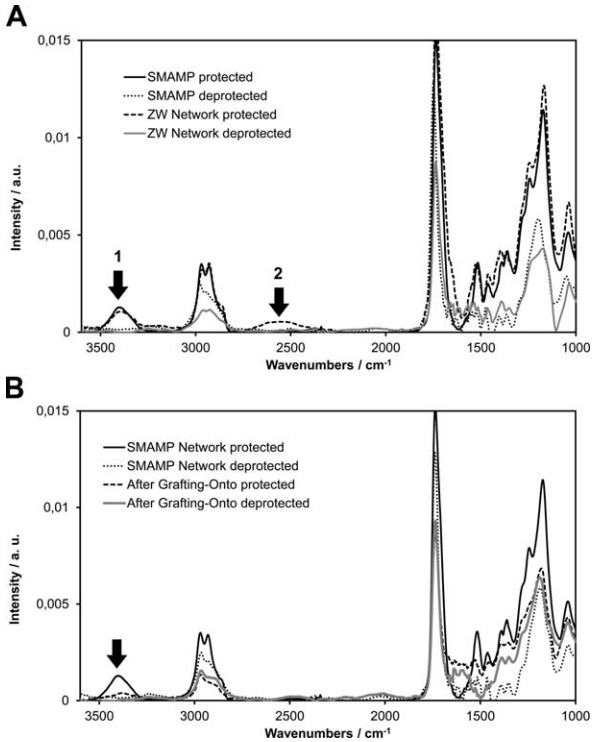

Fig. 7 FTIR-spectra of the target material and the two model surfaces. (a) SMAMP and poly(zwitterion) network in the protected and deprotected form. The NH stretch vibration of the Boc-group (arrow 1) and the OH stretch vibration of the COOH group (arrow 2) disappear after deprotection; (b) SMAMP network and the bifunctional material in the protected and deprotected form. Again, the NH stretch vibration vanishes after deprotection (arrow).

surface-immobilized as a network, onto which the end-functionalized poly(zwitterion) precursor was grafted. Deprotection yielded the antibiofouling poly(zwitterions) as "dangling arms" on a carpet of the antimicrobially active SMAMP. The material was characterized using ellipsometry, contact angle measurements, FTIR, AFM and SPR. The ellipsometry data and AFM measurements indicate a slight thickness increase, which hints at a thin layer of poly(zwitterions) on top of the SMAMP network. Contact angle measurements confirm the presence of such a layer, as the data of the pure poly(zwitterionic) sample and the bifunctional material almost coincide. These data are further backed up by the protein adhesion studies using SPR, as these measurements demonstrated that a pure SMAMP surface is strongly biofouling, while both the poly(zwitterion) network and the bifunctional surfaces are protein repellent when exposed to bovine serum albumin and fibrinogen, respectively. We therefore conclude that the synthesis of our target material was successful, and that a chemically robust surface containing SMAMPs and poly(zwitterions) was obtained.

To come back to the castle analogy, we have a strong indication that the walls of our castle, *i.e.* the antibiofouling moieties, are solid. It remains to be shown that the castle knights are also able to fulfill their task, *i.e.* we need to probe the antimicrobial activity, and study how these surfaces will perform in a "real" setting with immersion into bacterial suspensions for a long time. We will also determine how much of the antibiofouling

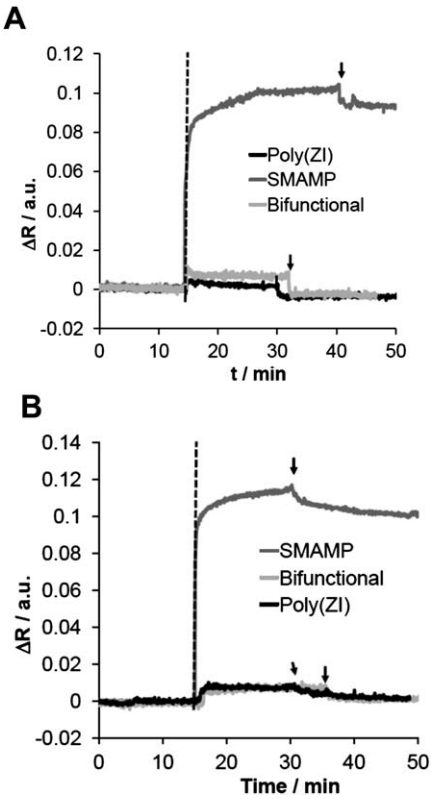

Fig. 8 Kinetic SPR measurement: the change in reflectivity upon exposure of the materials to a protein solution (A: BSA, B: fibrinogen) is plotted *versus* time. In both cases, the SMAMP is strongly fouling, whereas all protein can be flushed from both the poly(zwitterion) and the bifunctional material when buffer is injected.

component is needed to be sufficiently antibiofouling, while maintaining the antimicrobial activity. These experiments are underway, and we will report on them in due course.

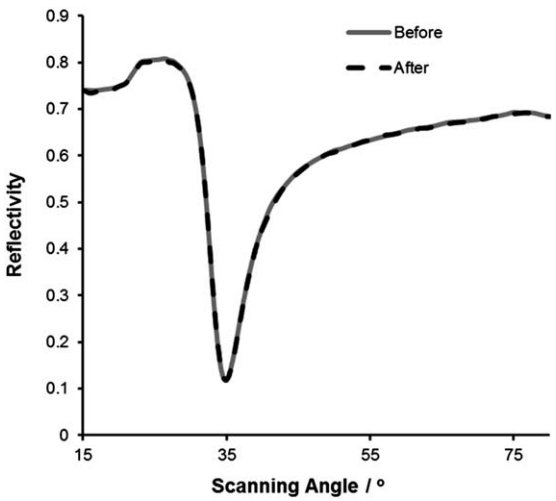

Fig. 9 Surface plasmon resonance curve (reflectivity in arbitrary units *vs.* scanning angle) measured before and after protein adsorption on the bifunctional material. The curves are identical for BSA and fibrinogen, indicating that, within the limit of the experimental method, no protein was adsorbed.

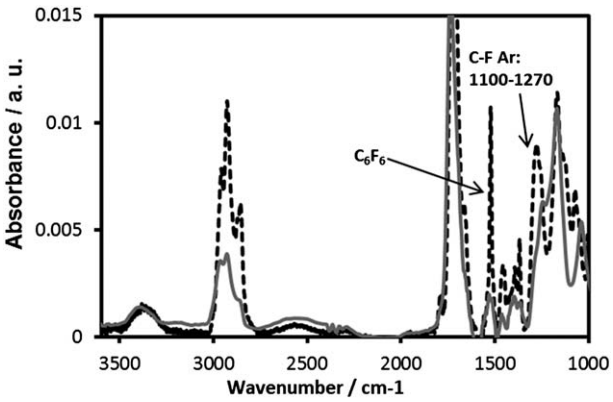

Fig. 10 FTIR-spectrum of the end-functionalized poly(zwitterion) (broken line) and the poly(zwitterion) network (solid line). The signals due to the pentafluorophenol end-group (arrows) are clearly observed.

Experimental

General

All chemicals were obtained as reagent grade from Aldrich, Fluka or Acros and used as received. HPLC grade solvents were purchased dry from Aldrich or Acros and used as received. Gel permeation chromatography (DMF/3 g L^{-1} LiCl, or chloroform, calibrated with polystyrene standards) was performed on a PSS GRAM or SDV column (PSS, Mainz, Germany). NMR spectra were recorded on a Bruker 250 MHz spectrometer (Bruker, Madison, WI, USA).

Ellipsometry

The thickness of the dry polymer layers on silicon wafers was measured with the auto-nulling imaging ellipsometer Nanofilm EP^3 (Nanofilm Technologie GmbH, Göttingen, Germany), which was equipped with a 532 nm solid-state laser. A refractive index of 1.5 was used for all measurements. For each sample, the average value from three different positions was taken.

FTIR spectrometry

To measure the Fourier-transform infrared (FTIR) spectra, the polymer layers were immobilized on one side of a double side polished silicon wafer. FTIR spectra were recorded with 64 scans using a Bio-Rad Excalibur spectrometer (Bio-Rad, München, Germany) between 4000 and 400 cm^{-1}. A spectrum of the blank double side polished silicon wafer was used as background.

Contact angle

The contact angles were measured with a contact angle system OCA 20 (Dataphysics GmbH, Filderstadt, Germany). Every contact angle measurement was repeated at four different points of the sample, and the average value was reported. The Laplace–Young method was used to calculate the static contact angles, while the advancing and receding contact angles were calculated with elliptical and tangent methods.

Atomic force microscopy

The morphology and roughness of the dry polymer layers on silicon wafers were measured after each step with a Multimode atomic force microscope (AFM) (Nanoscope IIIa, Digital Instruments, Santa Barbara, USA), which was equipped with commercial tips (AppNano). The resonance frequency of the tips was about 180 kHz, and the spring constant 20–95 N m^{-1}. All AFM micrographs were recorded in air under ambient conditions. The images were acquired at 512 sample points per line and 512 lines using a scan rate of 0.32 Hz. After capturing the images using the Nanoscope v531r1 software, they were analyzed using Gwyddion 2.26. For each sample, the root mean square (RMS) average roughness from three images of an area of 5 × 5 μm^2 at different positions was taken. The thickness of each layer was measured by scratching across the samples with a scalpel and scanning with the AFM across the scratch.

Surface plasmon resonance spectroscopy

An RT2005 spectrometer (Res-Tec, Framersheim, Germany) was used for surface plasmon resonance (SPR) measurements. Glass slides (LaSFN9 glass) coated with a 1 nm chromium adhesion layer and a 50 nm gold layer were also obtained from Res-Tec. To measure the dielectric constants of the polymer layer, a thick polymer film was immobilized on the gold substrate and the angular dependent reflectivity of light at the base of glass prism was recorded. The dielectric constants were calculated by fitting this reflection curve consisting of a plasmon surface polariton (PSP) and several guided optical waves (GOW) with the software Winspall 3.02 (Res-Tec). Any other layer thickness of the same polymer was then obtained by fitting the experimental reflection curve with these dielectric constants. To observe the protein adsorption on the polymer layer, first an angular dependent reflection curve was obtained after injecting PBS buffer solution (pH = 7.4). From this curve, the half-maximum angle on the left flank of the resonance signal was determined. The reflectivity as a function of time was then monitored at this angle (kinetic measurement). In a typical protein adsorption experiment, a protein (serum albumin or fibrinogen) in buffer was then injected into the SPR flow cell. After about 15 min, the flow cell was flushed with buffer. Any protein that would be irreversibly adsorbed on the surface would cause a shift in the resonance angle and lead to an increase of reflectivity in the kinetic measurement. Finally, the surface was dried under N_2-flow overnight and another angular dependent reflection curve was recorded to compare with the one before injection of buffer solution.

Synthesis

Synthesis of cross-linking agents. The cross-linking agent 3EBP-silane was synthesized as described in the literature.[31] The cross-linking agent DS (**11**) was synthesized using the following procedure (Scheme 1):

A solution of 4-hydroxybenzophenone (2.0 g, 10 mmol), lipoic acid (2.3 g, 11 mmol, 1.1 aq.) and DMAP (1.3 g, 11 mmol, 1.1 aq.) in anhydrous dichloromethane (DCM) was cooled in an ice bath under nitrogen. Dicyclohexyl carbodiimide (DCC) (2.3 g, 11 mmol, 1.1 aq.) was dissolved in 10 mL anhydrous DCM

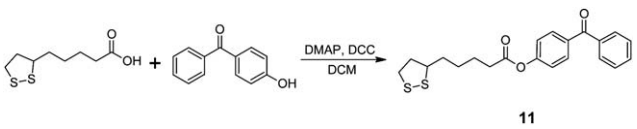

Scheme 1 Synthesis of the cross-linker DS.

and added within one hour. After stirring for 24 h at room temperature, the resulting urea byproduct was removed by filtration over a short silica gel column. The solvent was evaporated, and the crude product was purified by column chromatography (silica gel, ethyl acetate/*n*-hexane 1 : 3). The product **11** (2.4 g, 6.2 mmol, 62%) was obtained as a yellow solid. ^{1}H-NMR (250 MHz, $CDCl_3$): 1.60 (m, 2H, 4-CH_2), 1.72–1.85 (m, 4H, 3-CH_2 and 5-CH_2), 1.93 (dddd, 1H, 7-CH eq.), 2.48 (dddd, 1H, 7-CH ax.), 2.62 (t, 2H, 2-CH_2), 3.14 (m, 2H, 8-CH_2), 3.60 (ddt, 1H, 6-CH), 7.19–7.24 (m, 2H, 3″-CH and 5″-CH), 7.46–7.51 (m, 2H, 3′-CH and 5′-CH), 7.56–7.62 (m, 1H, 4″-CH), 7.78–7.82 (m, 2H, 2″-CH and 6″-CH), 7.83–7.88 (m, 2H, 2′-CH and 6′-CH). ^{13}C-NMR (62.9 MHz, $CDCl_3$): 25.0 (2-CH_2), 29.1 (4-CH_2), 34.6 (2-CH_2), 35.0 (5CH_2), 38.9 (8-CH_2), 40.7 (7-CH_2), 56.7 (6-CH), 121.9 (3″-CH),128.8 (2″-CH), 130.4 (3′-CH), 132.1 (2′-CH), 132.9 (4″-CH), 135.4 (1″-C), 137.9 (1′-C), 154.3 (4′-C-O), 171.9 (1-C═O), 195.9 (O═CPh_2).

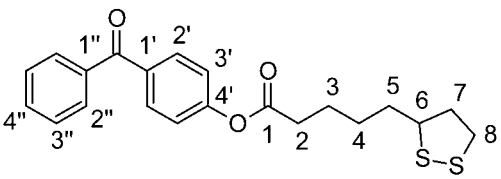

Synthesis of polymers

SMAMP precursor (Scheme 2): The antimicrobial SMAMP precursor **1** polymer was synthesized as described

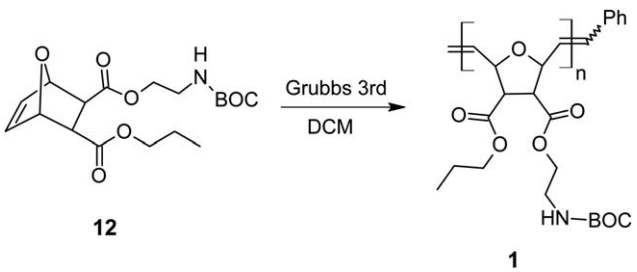

Scheme 2 Synthesis of the SMAMP precursor polymer.

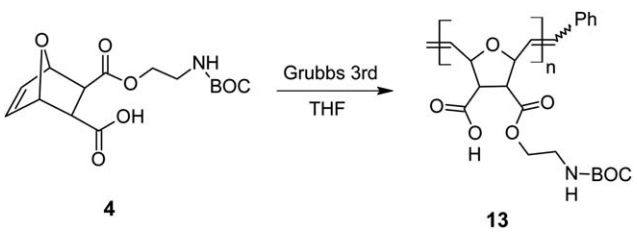

Scheme 3 Synthesis of the poly(zwitterion) precursor.

previously.[20m,22d,e] A typical polymerization was performed as follows, where all manipulations were performed under nitrogen using standard Schlenk techniques: monomer **12** (Scheme 2, 500 mg, 1.35 mmol) was dissolved in 2 mL CH_2Cl_2. Grubbs' third generation catalyst (3.6 mg, 5 μmol) was dissolved in 2 mL CH_2Cl_2 in a second flask and added to the monomer solution. After 30 min, an excess of ethylvinyl ether (1 mL) was added. The mixture was stirred for 2 hours. The solvent was then evaporated under reduced pressure. The NMR signals of the polymer **1** matched those in the literature.[22e] GPC analysis (PSS SDV column, chloroform, r.t., 1 mL min^{-1}) indicated that a polymer with a molecular weight of 120 000 g mol^{-1} and a polydispersity of 1.24 was obtained.

Antibiofouling precursor polymer ***13*** (Scheme 3). The antibiofouling monomer **4** (Scheme 3) was synthesized as described in the literature.[22c] The antibiofouling precursor polymer **13** was obtained analogously to the SMAMP synthesis. However, THF was used instead of DCM. In a typical experiment, 500 mg monomer **4** (1.2 mmol) and 3.7 mg Grubbs' third generation catalyst (5 μmol) were used. The NMR signals of the polymer **13** matched those in the literature.[22c]

Synthesis of the end-functionalization of the antibiofouling precursor polymer ***6*** (Fig. 4). Polymer **6** was synthesized by modification of an already published procedure for an end-functionalized SMAMP (Fig. 4), with a target molecular weight of 6000 g mol^{-1}.[22b] The protected zwitterionic monomer **4** (500 mg, 1.5 mmol) was dissolved in 5 mL DCM under nitrogen. Grubbs' third generation catalyst (60.7 mg, 0.08 mmol) was dissolved in a second flask in 2 mL DCM under nitrogen. Both solutions were stirred at room temperature for 30 min. The monomer solution was then added to the catalyst and the mixture was stirred for another 30 min. The pentafluorophenol end group **5** (94.2 mg, 0.16 mmol) was dissolved in 2 mL DCM and added to the reaction mixture. After stirring for 24 hours, the unreacted end group was removed by washing with 500 mL DCM over an Al_2O_3 column. The polymer, which remained on top of the column, was then washed out with ethyl acetate. The product **6** was obtained after evaporation of the solvent. ^{1}H-NMR (250 MHz, $CDCl_3$): 1.45 (s, 9H, 3 × 9-CH_3), 2.94 (t, 0.1H, 3″-CH_2), 3.13 (br m, 2H, 3- and 3′-CH), 3.32 (br m, 2H, 6-CH_2), 3.83 (t, 0.1H, 4″-CH_2), 4.06 (m, 0.1H, 2″-CH_2), 4.21 (m, 2H, 5-CH_2), 4.76 (br m, 1H, 2- and 2′ trans-H), 5.10 (br s, 1H, NH), 5.64 (br m, 1H, 2 *cis*- and 2′-H), 5.83 (br m, 1H, 1- and 1′ *cis*-H), 5.92 (br m, 1H, 1- and 1′ trans-H), 6.76–7.10 (m, phenyl end-group). GPC (PSS GRAM column DMF/3 g L^{-1} LiCl, 1 mL min^{-1}): M_n = 4400 g mol^{-1}, M_w = 5800 g mol^{-1}, M_w/M_n = 1.3; FTIR-data: Fig. 10.

Functionalization of the silicon wafer and gold substrate with cross-linking agents

Silicon wafer. A solution of 3EBP-silane (20 mg mL^{-1} in toluene) was spin coated on a (525 ± 25) μm thick one-side-polished 100 mm standard Si (CZ) wafer ([100] orientation, 1000 rpm, 120 s). The wafer was cured for 30 min at 100 °C on a preheated hot plate, washed with toluene and dried under a continuous flow of nitrogen.

Gold. For SPR measurements, the LaSFN9 glass slides coated with 1 nm chromium and a 50 nm gold layer were covered with a 5 mM solution of DS in toluene for 24 h. Then the samples were washed with toluene and ethanol, and dried under nitrogen flow. SPR measurements indicated that the thickness of the DS layer was 2 nm.

Immobilization of polymer networks on silicon wafers and gold substrates functionalized with benzophenone

SMAMP precursor network 7 and SMAMP network ***8****.* A solution of polymer **1** (10 mg mL^{-1}), pentaerythritol-tetrakis-(3-mercaptopropionate) (= tetrathiol **2**, 0.04 mg mL^{-1}) and 2,2-dimethoxy-2-phenylaceto-phenone (DMPAP **3**, 0.01 mg mL^{-1}) in a mixture of DCM and toluene (1 : 4) was produced. From this solution, a polymer film was spin cast on a 3-EBP treated silicon wafer or DS treated gold substrate at 3000 rpm for 2 min. The film was cross-linked at 254 nm for 30 min in a BIO-LINK Box (Vilber Lourmat GmbH). It was then washed with dichloromethane to remove unattached polymer chains and dried overnight under N_2-flow. This yielded the precursor network **7**. To activate the antimicrobial function, the film was immersed in HCl (4 M in dioxane) for 12 hours and washed twice with ethanol. It was then dried overnight under N_2-flow to yield the SMAMP network **8**.

Poly(zwitterion) network. A solution with the same concentration was made from polymer **13**, tetrathiol and DMPAP in a mixture of THF and toluene (1 : 4). The remaining steps were exactly the same as described above for the polymer network **8**.

Grafting-onto reaction on the SMAMP polymer layer 8. A silicon wafer (1.5 × 1.5 cm) or a gold substrate was modified with an antimicrobial polymer network **8** as described above. After deprotection, it was placed into a vial, which was previously dried and filled with N_2. The wafer was then covered with a solution of the end-functionalized poly(zwitterion) **6** (6 mg, 1×10^{-3} mmol, M = 6000 g mol^{-1}) in 4 mL DCM. A solution of DMAP in DCM (1 mL, 0.24 mg mL^{-1}, 2 eq.) and then after 2 h a solution of DCC in DCM (1 mL, 0.42 mg mL^{-1}, 2 eq.) were added to the reaction mixture. After 3 days, the wafer was washed with hexane, DCM, water and ethanol to yield **9**. For deprotection of the Boc-group, the wafer was immersed in HCl (4 M in dioxane) for 5 h and washed twice with ethanol. Finally, the sample was dried under N_2-flow overnight. This yielded the bifunctional material **10**.

Acknowledgements

We would like to thank Jürgen Rühe and Oswald Prucker for helpful discussions. We also thank Franziska Dorner for revising the manuscript. Zhouling Deng, Natalia Schatz, and Alexander Dietz are gratefully acknowledged for experimental and technical assistance. Funding was received from the Freiburg Institute for Advanced Studies (FRIAS Junior Fellowship) and the Emmy-Noether program of the German Research Foundation (DFG, LI1714/5-1).

References

1 S. Krishnan, C. J. Weinman and C. K. Ober, *J. Mater. Chem.*, 2008, **18**, 3405–3413.

2 (*a*) A. Hucknall, S. Rangarajan and A. Chilkoti, *Adv. Mater.*, 2009, **21**, 2441–2446; (*b*) J. A. Lichter, K. J. Van Vliet and M. F. Rubner, *Macromolecules*, 2009, **42**, 8573–8586.

3 L. Hall-Stoodley, J. W. Costerton and P. Stoodley, *Nat. Rev. Microbiol.*, 2004, **2**, 95–108.

4 P. S. Stewart and J. W. Costerton, *Lancet*, 2001, **358**, 135–138.

5 (*a*) S. Schilp, A. Kueller, A. Rosenhahn, M. Grunze, M. E. Pettitt, M. E. Callow and J. A. Callow, *Biointerphases*, 2007, **2**, 143–150; (*b*) H. Ma, J. Hyun, P. Stiller and A. Chilkoti, *Adv. Mater.*, 2004, **16**, 338–341; (*c*) H. Du, P. Chandaroy and S. W. Hui, *Biochim. Biophys. Acta, Biomembr.*, 1997, **1326**, 236–248; (*d*) K. D. Park, Y. S. Kim, D. K. Han, Y. H. Kim, E. H. B. Lee, H. Suh and K. S. Choi, *Biomaterials*, 1998, **19**, 851–859; (*e*) V. E. Wagner, J. T. Koberstein and J. D. Bryers, *Biomaterials*, 2004, **25**, 2247–2263; (*f*) X. W. Fan, L. J. Lin and P. B. Messersmith, *Biomacromolecules*, 2006, **7**, 2443–2448; (*g*) G. Cheng, Z. Zhang, S. Chen, J. D. Bryers and S. Jiang, *Biomaterials*, 2007, **28**, 4192–4199; (*h*) S. Tugulu and H.-A. Klok, *Biomacromolecules*, 2008, **9**, 906–912; (*i*) K. Page, M. Wilson and I. P. Parkin, *J. Mater. Chem.*, 2009, **19**, 3819–3831.

6 H. Jiang, S. Manolache, A. C. Wong and F. S. Denes, *J. Appl. Polym. Sci.*, 2006, **102**, 2324–2337.

7 R. Konradi, B. Pidhatika, A. Muhlebach and M. Textort, *Langmuir*, 2008, **24**, 613–616.

8 (*a*) J. Ladd, Z. Zhang, S. Chen, J. C. Hower and S. Jiang, *Biomacromolecules*, 2008, **9**, 1357–1361; (*b*) Z. Zhang, H. Vaisocherova, G. Cheng, W. Yang, H. Xue and S. Jiang, *Biomacromolecules*, 2008, **9**, 2686–2692; (*c*) G. Cheng, G. Li, H. Xue, S. Chen, J. D. Bryers and S. Jiang, *Biomaterials*, 2009, **30**, 5234–5240; (*d*) S. Jiang and Z. Cao, *Adv. Mater.*, 2010, **22**, 920–932.

9 (*a*) A. L. Lewis, *Colloids Surf., B*, 2000, **18**, 261–275; (*b*) R. Iwata, P. Suk-In, V. P. Hoven, A. Takahara, K. Akiyoshi and Y. Iwasaki, *Biomacromolecules*, 2004, **5**, 2308–2314; (*c*) S. F. Rose, S. Okere, G. W. Hanlon, A. W. Lloyd and A. L. Lewis, *J. Mater. Sci.: Mater. Med.*, 2005, **16**, 1003–1015; (*d*) K. Hirota, K. Murakami, K. Nemoto and Y. Miyake, *FEMS Microbiol. Lett.*, 2005, **248**, 37–45; (*e*) T. Goda, T. Konno, M. Takai, T. Moro and K. Ishihara, *Biomaterials*, 2006, **27**, 5151–5160; (*f*) T. Goda, T. Konno, M. Takai and K. Ishihara, *Colloids Surf., B*, 2007, **54**, 67–73; (*g*) R. Iwata, R. Satoh, Y. Iwasaki and K. Akiyoshi, *Colloids Surf., B*, 2008, **62**, 288–298; (*h*) K. Bertal, J. Shepherd, C. W. I. Douglas, J. Madsen, A. Morse, S. Edmondson, S. P. Armes, A. Lewis and S. MacNeil, *J. Mater. Sci.*, 2009, **44**, 6233–6246; (*i*) K. Kitano, Y. Inoue, R. Matsuno, M. Takai and K. Ishihara, *Colloids Surf., B*, 2009, **74**, 350–357; (*j*) K. Yoshimoto, T. Hirase, J. Madsen, S. P. Armes and Y. Nagasaki, *Macromol. Rapid Commun.*, 2009, **30**, 2136–2140.

10 (*a*) Z. Zhang, S. Chen, Y. Chang and S. Jiang, *J. Phys. Chem. B*, 2006, **110**, 10799–10804; (*b*) Z. Zhang, T. Chao, S. Chen and S. Jiang, *Langmuir*, 2006, **22**, 10072–10077; (*c*) S. Colak and G. N. Tew, *Macromolecules*, 2008, **41**, 8436–8440; (*d*) G. Garg, G. S. Chauhan, R. Gupta and J. H. Ahn, *J. Colloid Interface Sci.*, 2010, **344**, 90–96.

11 (*a*) Z. Zhang, S. Chen and S. Jiang, *Biomacromolecules*, 2006, **7**, 3311–3315; (*b*) H. Vaisocherova, W. Yang, Z. Zhang, Z. Cao, G. Cheng, M. Piliarik, J. Homola and S. Jiang, *Anal. Chem.*, 2008, **80**, 7894–7901; (*c*) Z. Zhang, G. Cheng, L. R. Carr, H. Vaisocherova, S. F. Chen and S. Y. Jiang, *Biomaterials*, 2008, **29**, 4719–4725; (*d*) S. Tada, C. Inaba, K. Mizukami, S. Fujishita, M. Gemmei-Ide, H. Kitano, A. Mochizuki, M. Tanaka and T. Matsunaga, *Macromol. Biosci.*, 2009, **9**, 63–70; (*e*) W. Yang, L. Zhang, S. Wang, A. D. White and S. Jiang, *Biomaterials*, 2009, **30**, 5617–5621; (*f*) C. L. Gao, G. Z. Li, H. Xue, W. Yang, F. B. Zhang and S. Y. Jiang, *Biomaterials*, 2010, **31**, 1486–1492; (*g*) S. Y. Jiang and Z. Q. Cao, *Adv. Mater.*, 2010, **22**, 920–932.

12 (*a*) H. Kitano, A. Kawasaki, H. Kawasaki and S. Morokoshi, *J. Colloid Interface Sci.*, 2005, **282**, 340–348; (*b*) H. Kitano, S. Tada, T. Mori, K. Takaha, M. Gemmei-Ide, M. Tanaka, M. Fukuda and Y. Yokoyama, *Langmuir*, 2005, **21**, 11932–11940; (*c*) S. F. Chen, L. Y. Liu and S. Y. Jiang, *Langmuir*, 2006, **22**, 2418–2421; (*d*) H. Kitano, K. Nagaoka, S. Tada and M. Gemmei-Ide, *J. Colloid Interface Sci.*, 2007, **313**, 461–468.

13 S. Colak and G. N. Tew, *Langmuir*, 2012, **28**, 666–675.

14 E. M. Hetrick and M. H. Schoenfisch, *Chem. Soc. Rev.*, 2006, **35**, 780–789.

15 (*a*) J. C. Tiller, C. J. Liao, K. Lewis and A. M. Klibanov, *Proc. Natl. Acad. Sci. U. S. A.*, 2001, **98**, 5981–5985; (*b*) J. C. Tiller, S. B. Lee, K. Lewis and A. M. Klibanov, *Biotechnol. Bioeng.*, 2002, **79**, 465–471; (*c*) J. Lin, J. C. Tiller, S. B. Lee, K. Lewis and A. M. Klibanov, *Biotechnol. Lett.*, 2002, **24**, 801–805; (*d*) J. Lin, S. Y. Qiu, K. Lewis and A. M. Klibanov, *Biotechnol. Bioeng.*, 2003, **83**, 168–172; (*e*) J. Lin, S. Y. Qiu, K. Lewis and A. M. Klibanov, *Biotechnol. Prog.*, 2002, **18**, 1082–1086; (*f*) D. Park, J. Wang and A. M. Klibanov, *Biotechnol. Prog.*, 2006, **22**, 584–589; (*g*) N. M. Milovic, J. Wang, K. Lewis and A. M. Klibanov, *Biotechnol. Bioeng.*, 2005, **90**, 715–722.

16 (*a*) L. Cen, K. G. Neoh and E. T. Kang, *Langmuir*, 2003, **19**, 10295–10303; (*b*) L. Cen, K. G. Neoh and E. T. Kang, *J. Biomed. Mater. Res.*, 2004, **71A**, 70–80; (*c*) F. X. Hu, K. G. Neoh, L. Cen and E. T. Kang, *Biotechnol. Bioeng.*, 2005, **89**, 474–484; (*d*) A. D. Fuchs and J. C. Tiller, *Angew. Chem., Int. Ed.*, 2006, **45**, 6759–6762.

17 J. Thome, A. Hollander, W. Jaeger, I. Trick and C. Oehr, *Surf. Coat. Technol.*, 2003, **174**, 584–587.

18 A. E. Madkour, J. A. Dabkowski, K. Nusslein and G. N. Tew, *Langmuir*, 2009, **25**, 1060–1067.

19 (*a*) S. B. Lee, R. R. Koepsel, S. W. Morley, K. Matyjaszewski, Y. J. Sun and A. J. Russell, *Biomacromolecules*, 2004, **5**, 877–882; (*b*) J. Y. Huang, H. Murata, R. R. Koepsel, A. J. Russell and K. Matyjaszewski, *Biomacromolecules*, 2007, **8**, 1396–1399; (*c*) H. Murata, R. R. Koepsel, K. Matyjaszewski and A. J. Russell, *Biomaterials*, 2007, **28**, 4870–4879.

20 (*a*) E. A. Porter, X. F. Wang, H. S. Lee, B. Weisblum and S. H. Gellman, *Nature*, 2000, **404**, 565; (*b*) D. H. Liu and W. F. DeGrado, *J. Am. Chem. Soc.*, 2001, **123**, 7553–7559; (*c*) T. L. Raguse, E. A. Porter, B. Weisblum and S. H. Gellman, *J. Am. Chem. Soc.*, 2002, **124**, 12774–12785; (*d*) G. N. Tew, D. H. Liu, B. Chen, R. J. Doerksen, J. Kaplan, P. J. Carroll, M. L. Klein and W. F. DeGrado, *Proc. Natl. Acad. Sci. U. S. A.*, 2002, **99**, 5110–5114; (*e*) J. A. Patch and A. E. Barron, *Curr. Opin. Chem. Biol.*, 2002, **6**, 872–877; (*f*) D. H. Liu, S. Choi, B. Chen, R. J. Doerksen, D. J. Clements, J. D. Winkler, M. L. Klein and W. F. DeGrado, *Angew. Chem., Int. Ed.*, 2004, **43**, 1158–1162; (*g*) K. Kuroda and W. F. DeGrado, *J. Am. Chem. Soc.*, 2005, **127**, 4128–4129; (*h*) H. Tang, R. J. Doerksen, T. V. Jones, M. L. Klein and G. N. Tew, *Chem. Biol.*, 2006, **13**, 427–435; (*i*) I. Ivanov, S. Vemparala, V. Pophristic, K. Kuroda, W. F. DeGrado, J. A. McCammon and M. L. Klein, *J. Am. Chem. Soc.*, 2006, **128**, 1778–1779; (*j*) K. Lienkamp, A. E. Madkour, A. Musante, C. F. Nelson, K. Nusslein and G. N. Tew, *J. Am. Chem. Soc.*, 2008, **130**, 9836–9843; (*k*) G. J. Gabriel, J. G. Pool, A. Som, J. M. Dabkowski, E. B. Coughlin, M. Muthukurnar and G. N. Tew, *Langmuir*, 2008, **24**, 12489–12495; (*l*) G. J. Gabriel, J. A. Maegerlein, C. E. Nelson, J. M. Dabkowski, T. Eren, K. Nusslein and G. N. Tew, *Chem.–Eur. J.*, 2009, **15**, 433–439; (*m*) K. Lienkamp, A. E. Madkour, K. N. Kumar, K. Nusslein and G. N. Tew, *Chem.–Eur. J.*, 2009, **15**, 11715–11722; (*n*) K. Lienkamp and G. N. Tew, *Chem.–Eur. J.*, 2009, **15**, 11784–11800; (*o*) B. P. Mowery, A. H. Lindner, B. Weisblum, S. S. Stahl and S. H. Gellman, *J. Am. Chem. Soc.*, 2009, **131**, 9735–9745; (*p*) K. Kuroda, G. A. Caputo and W. F. DeGrado, *Chem.–Eur. J.*, 2009, **15**, 1123–1133; (*q*) G. N. Tew, R. W. Scott, M. L. Klein and W. F. Degrado, *Acc. Chem. Res.*, 2010, **43**, 30–39.

21 (*a*) J. Lin, S. Qiu, K. Lewis and A. M. Klibanov, *Biotechnol. Bioeng.*, 2003, **83**, 168–172; (*b*) A. M. Klibanov, *J. Mater. Chem.*, 2007, **17**, 2479–2482; (*c*) S. Krishnan, R. J. Ward, A. Hexemer, K. E. Sohn, K. L. Lee, E. R. Angert, D. A. Fischer, E. J. Kramer and C. K. Ober, *Langmuir*, 2006, **22**, 11255–11266; (*d*) J. Y. Huang, R. R. Koepsel, H. Murata, W. Wu, S. B. Lee, T. Kowalewski, A. J. Russell and K. Matyjaszewski, *Langmuir*, 2008, **24**, 6785–6795; (*e*) H. Nikaido and T. Nakae, *Adv. Microb. Physiol.*, 1979, **20**, 163–250; (*f*) R. Kugler, O. Bouloussa and F. Rondelez, *Microbiology*, 2005, **151**, 1341–1348; (*g*) J. C. Tiller, G. Bonner, L. C. Pan and A. M. Klibanov, *Biotechnol. Bioeng.*, 2001, **73**, 246–252.

22 (*a*) G. N. Tew, A. E. Madkour, K. Lienkamp and A. M. Musante, Application: WO2010144386, University of Massachusetts, USA, 2010, p. 146; (*b*) A. E. Madkour, A. H. R. Koch, K. Lienkamp and G. N. Tew, *Macromolecules*, 2010, **43**, 4557–4561; (*c*) K. Lienkamp, A. E. Madkour, K.-N. Kumar, K. Nuesslein and G. N. Tew, *Chem.–Eur. J.*, 2009, **15**, 11715–11722, S11715/11711-S11715/11713;

(*d*) K. Lienkamp, K.-N. Kumar, A. Som, K. Nüsslein and G. N. Tew, *Chem.–Eur. J.*, 2009, **15**, 11710–11714; (*e*) K. Lienkamp, A. E. Madkour, A. Musante, C. F. Nelson, K. Nüsslein and G. N. Tew, *J. Am. Chem. Soc.*, 2008, **130**, 9836–9843.
23 S. K. Jewrajka and S. Haldar, *Polym. Compos.*, 2011, **32**, 1851–1861.
24 (*a*) D.-S. Kim, S. B. Jagani and D.-Y. Yoon, *AIChE Annual Meeting*, Conference Proceedings, Nashville, TN, United States, November 8–13 2008, vol. 2009, pp. 591–592; (*b*) V. R. Sendamangalam, D. S. Kim and Y. Seo, *Abstracts of Papers, 239th ACS National Meeting*, San Francisco, CA, United States, March 21–25 2010, vol. 2010, ENVR-4.
25 J. Xue, L. Chen, H. L. Wang, Z. B. Zhang, X. L. Zhu, E. T. Kang and K. G. Neoh, *Langmuir*, 2008, **24**, 14151–14158.
26 A. Vora and Y.-H. La, *Polym. Prepr. (Am. Chem. Soc., Div. Polym. Chem.)*, 2011, **52**, 1072–1073.
27 (*a*) G. Cheng, Q. Tang and Y. Chen, *Abstracts of Papers, 241st ACS National Meeting & Exposition*, Anaheim, CA, United States, March 27-31 2011, vol. 2011, CARB-59; (*b*) G. Cheng, H. Xite, Z. Zhang, S. F. Chen and S. Y. Jiang, *Angew. Chem., Int. Ed.*, 2008, **47**, 8831–8834.
28 S. Jiang, *Abstracts of Papers, 243rd ACS National Meeting & Exposition*, San Diego, CA, United States, March 25–March 29 2012, vol. 2012, COLL-555.
29 Z. Cao, L. Mi, J. Mendiola, J.-R. Ella-Menye, L. Zhang, H. Xue and S. Jiang, *Angew. Chem., Int. Ed.*, 2012, **51**, 2602–2605, S2602/2601-S2602/2608.
30 O. Prucker, C. A. Naumann, J. Rühe, W. Knoll and C. W. Frank, *J. Am. Chem. Soc.*, 1999, **121**, 8766–8770.
31 M. Gianneli, R. F. Roskamp, U. Jonas, B. Loppinet, G. Fytas and W. Knoll, *Soft Matter*, 2008, **4**, 1443–1447.